

Charge compensation and optimal stoichiometry in superconducting (Ca_xLa_{1-x})(Ba_{1.75-x}La_{0.25+x})Cu₃O_y

Dale R. Harshman^{1,2,*} and Anthony T. Fiory³

¹ *Physikon Research Corporation, Lynden, Washington 98264, USA*

² *Department of Physics, University of Notre Dame, Notre Dame, Indiana 46556, USA*

³ *Department of Physics, New Jersey Institute of Technology, Newark, New Jersey 07102, USA*

(25 October 2012)

The superconductive and magnetic properties of charge-compensated (Ca_xLa_{1-x})(Ba_{1.75-x}La_{0.25+x})Cu₃O_y (normally denoted as CLBLCO) are considered through quantitative examination of data for electrical resistivity, magnetic susceptibility, transition width, muon-spin rotation, x-ray absorption, and crystal structure. A derivative of LaBa₂Cu₃O_y, cation doping of this unique tetragonal cuprate is constrained by compensating La substitution for Ba with Ca substitution for La, where for $0 \leq x \leq 0.5$ local maxima in T_C occur for y near 7.15. It is shown that optimum superconductivity occurs for $0.4 \leq x \leq 0.5$, that the superconductivity and magnetism observed are nonsymbiotic phenomena, and that charge-compensated doping leaves the carrier density in the cuprate planes nearly invariant with x , implying that only a small fraction of superconducting condensate resides therein. Applying a model of electronic interactions between physically separated charges in adjacent layers, the mean in-plane spacing between interacting charges, $\ell = 7.1206 \text{ \AA}$, and the distance between interacting layers, $\zeta = 2.1297 \text{ \AA}$, are determined for $x = 0.45$. The theoretical optimal $T_{C0} \propto \ell^{-1}\zeta^{-1}$ of 82.3 K is in excellent agreement with experiment ($\approx 80.5 \text{ K}$), bringing the number of compounds for which T_{C0} is accurately predicted to 37 from six different superconductor families (overall accuracy of $\pm 1.35 \text{ K}$).

Keywords: High- T_C superconductivity theory, charge compensated, Coulomb mediated pairing

DOI: [10.1103/PhysRevB.86.144533](https://doi.org/10.1103/PhysRevB.86.144533)

PACS number(s): 74.20.-z, 74.62.-c, 74.72.-h

I. INTRODUCTION

The charge-compensated compound (Ca_xLa_{1-x})(Ba_{c-x}La_{2.0-c+x})Cu₃O_y with $c = 1.75$ is a derivative of LaBa₂Cu₃O_{7- δ} wherein $(0.25 + x)$ La⁺³ substituting for Ba⁺², coupled with (x) Ca⁺² substituting for the La⁺³ separating the cuprate planes, preserves a constant cation charge value (exclusive of the Cu ions) of $Q = +7.25$,¹ hence the “charge-compensated” denotation. Early experiments exploring the c - x - y formulation matrix determined a maximum transition temperature of $T_C^{\max} = 82 \text{ K}$ by studying the dependence of y relative to the metal-insulator transition value y_{M-I} .² Subsequent investigations provided more detail on the y dependence of T_C , and nearly the same $T_C^{\max} = 81 \text{ K}$ occurs for $x = 0.4$, and y in the vicinity of 7.15.^{3,4} The authors of Ref. 2 obtained a unique experimental result that corresponds to the optimum T_{C0} , as defined in Ref.

5 and herein. The later researchers^{3,4,6} introduce a different scaling phenomenology: y is offset by a model function of x and T_C is scaled to a redefined T_C^{\max} that depends on x (this redefinition is discussed further in Sec. IV).

For (Ca_xLa_{1-x})(Ba_{1.75-x}La_{0.25+x})Cu₃O_y, the optimal superconductive material is most closely realized by the stoichiometry corresponding to T_C^{\max} (as originally defined²). Deviations from optimum stoichiometry (yielding $T_C < T_{C0}$) typically introduce inhomogeneities which degrade the superconductive quality of the material, manifested as depressed resistive superconducting transitions (considered generally in Refs. 7 and 8). For example, maintaining a constant Q by controlling the average cation valence does not prevent changes in the charge available for superconductivity, nor the degradation of the

superconducting condensate caused by widely varying c , x or y from their optimum values. Consequently, $(\text{Ca}_x\text{La}_{1-x})(\text{Ba}_{1.75-x}\text{La}_{0.25+x})\text{Cu}_3\text{O}_y$ materials grown with $x < 0.4$, as shown by the data presented in Sec. II, are nonoptimal.

Owing to the charge-compensated nature of $(\text{Ca}_x\text{La}_{1-x})(\text{Ba}_{1.75-x}\text{La}_{0.25+x})\text{Cu}_3\text{O}_y$, it is instructive to consider the optimal material (achieved for $0.4 \leq x \leq 0.5$) from the perspective of a new theoretical treatment that assumes the pairing is mediated via Coulomb interactions between physically separated carrier bands;⁵ $\text{YBa}_2\text{Cu}_3\text{O}_{7-\delta}$ (90-K phase optimized for $\delta = 0.08$) and other optimal high- T_C compounds have been found to contain both holes and electrons confined in two dimensions and separated physically in different regions of the unit cell.^{9,10} From this, and the fact that phonon (or polaron) mediation has been ruled out,¹¹ it is natural to expect that Coulomb forces between the holes and electrons would dominate the superconductive pairing. At the time of this writing, this model has been validated (with a statistical error between the calculated and measured T_{C0} of ± 1.34 K) for 36 different materials from six superconducting families (cuprates, ruthenates, rutheno-cuprates, iron pnictides, iron chalcogenides, and organics), with measured T_{C0} values ranging from 10 K to 150 K.^{12,13} The present application of this model to $(\text{Ca}_x\text{La}_{1-x})(\text{Ba}_{1.75-x}\text{La}_{0.25+x})\text{Cu}_3\text{O}_y$ gives $T_{C0} = 82.3$ K (see Sec. III).

Section II presents an analysis of prior experimental data to help clarify the unique experimental result identifying T_C^{max} for $(\text{Ca}_x\text{La}_{1-x})(\text{Ba}_{1.75-x}\text{La}_{0.25+x})\text{Cu}_3\text{O}_y$, showing that the optimal charge-compensation variable x lies in the range 0.4 to 0.5. Relevant observations include the nonproportional variation between nonoptimum T_C and muon-spin depolarization rate, nuclear quadrupole resonance (NQR) frequencies, and x-ray absorption spectroscopy (XAS) measurements of cuprate-plane charges showing a near invariance with x . In Sec. III, the theory for T_{C0} derived from pairing by the interlayer Coulomb interaction between physically separated charge layers is briefly described, and T_{C0} for optimal $(\text{Ca}_x\text{La}_{1-x})(\text{Ba}_{1.75-x}\text{La}_{0.25+x})\text{Cu}_3\text{O}_y$ is calculated. Section IV provides discussions of oxygen stoichiometry, superconducting inhomogeneity and locus, magnetic behavior, and the measurements-based rationale for distinguishing between optimum and non-optimum materials. Conclusions are drawn in Sec. V.

II. SUMMARY OF EXPERIMENTAL RESULTS

Early electrical resistivity and magnetic susceptibility data on $(\text{Ca}_x\text{La}_{1-x})(\text{Ba}_{1.75-x}\text{La}_{0.25+x})\text{Cu}_3\text{O}_y$, measured as functions of x and y , clearly exhibit non-optimal behavior for $x < 0.4$ and for any value of y . The experimental evidence includes transition temperatures T_C^R and T_C^Z , and associated transition widths ΔT_C^R and ΔT_C^Z , from resistivity and susceptibility, respectively, for values of x ranging from 0 to 0.50 and $y \approx 7.1$.¹ Later results were obtained from superconducting onset constructions that typically yield higher transition points.^{2,4} The various measurements of the highest (or nearly the highest) transition temperature at each x are plotted as functions of x in Fig. 1, illustrating the trend: for $x \sim 0.45$ to 0.50, T_C is maximum and approaches the T_C^{max} of 82 K reported in Ref. 2 and 81 K reported in Refs. 3 and 4. Also marked in Fig. 1 is the T_{C0} calculated in Sec. III B, which nearly coincides with the observed maximum T_C .

The inset in Fig. 1 shows that there is a finite pressure dependence of T_C ($dT_C/dP > 0$),² which introduces some uncertainty in establishing an upper bound for T_C^{max} . That dT_C/dP turns sharply downward

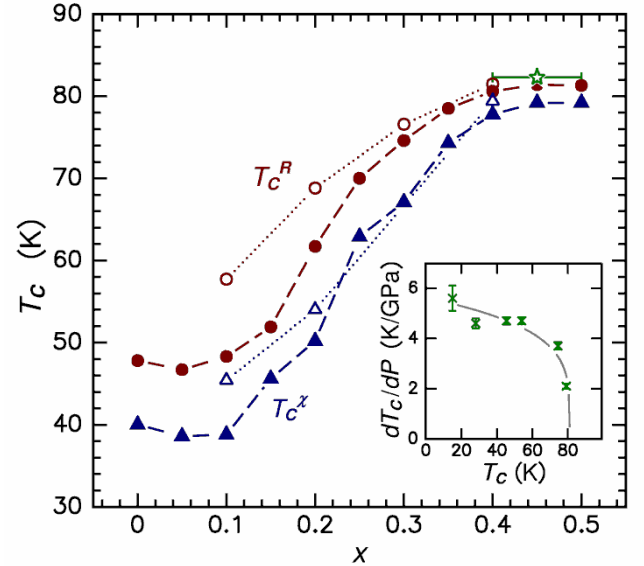


FIG. 1. Transition temperatures T_C for $(\text{Ca}_x\text{La}_{1-x})(\text{Ba}_{1.75-x}\text{La}_{0.25+x})\text{Cu}_3\text{O}_y$, maximized by oxygen content y , extracted from electrical resistivity (filled circles after Ref. 1, open circles after Ref. 4) and magnetic susceptibility (filled triangles after Ref. 1, open triangles after Ref. 2) as a function of x . Star symbol denotes theoretical T_{C0} averaged over $x = 0.4 - 0.5$. Inset represents dT_C/dP vs T_C after Ref. 2; curve denotes trend.

as T_C approaches T_C^{\max} suggests that any pressure correction on the extrapolated T_C^{\max} is likely to be small.

Specific experimental indicators of materials quality are extractable from temperature-dependent resistivity $\rho(T)$. By fitting a line to $\rho(T)$ just above T_C (using data plotted in Ref. 1 for analysis), the extrapolated normal-state resistivity at T_C , denoted as $\rho(T_C^+)$, and the extrapolated zero-temperature residual resistivity, denoted as $\rho(0)$, have been determined in this work. These resistivity data together with the associated percentage transition widths $\Delta T_C/T_C$ are plotted in Fig. 2. Viewed as functions of x , it is clear that the extrapolated $\rho(0)$ trends from large values at low x to very small values in the vicinity of $x \sim 0.45$ to 0.50, signaling that T_C^{\max} corresponds to minimization of electronic scattering and disorder. The similar downward trend of the normal-state resistivity, represented by $\rho(T_C^+)$, to values under 0.5 m Ω cm indicates a corresponding approach to good metal transport. The associated decreasing trend in $\Delta T_C/T_C$ shows that samples for $x \geq 0.4$ have the most uniform superconducting states, which is consistent with the indicators of lowest disorder from normal-state transport.

Superconductivity in $(\text{Ca}_x\text{La}_{1-x})(\text{Ba}_{1.75-x}\text{La}_{0.25+x})\text{Cu}_3\text{O}_y$ has also been qualified for various x and y by means of positive muon-spin-rotation spectroscopy

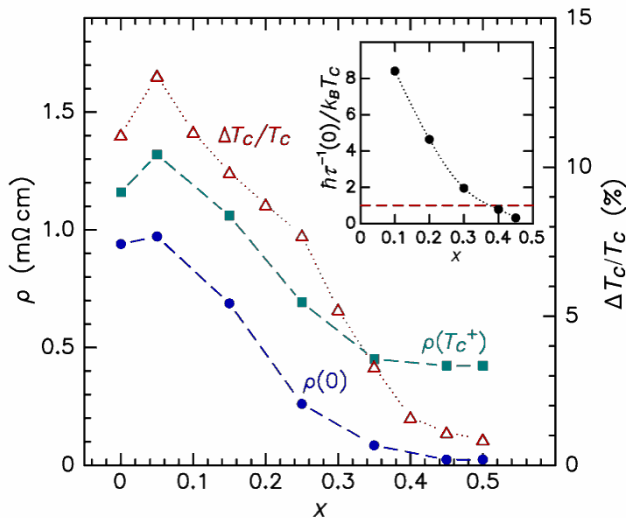


FIG. 2. Resistivity measurements $\rho(T_C^+)$ and $\rho(0)$, left scale, and the percentage transition widths $\Delta T_C/T_C$, right scale, plotted as functions of x for $(\text{Ca}_x\text{La}_{1-x})(\text{Ba}_{1.75-x}\text{La}_{0.25+x})\text{Cu}_3\text{O}_y$, with y set to maximize T_C (after Ref. 1). Inset shows $\hbar\tau^{-1}(0)/k_B T_C$ plotted against doping x ; horizontal dashed line denotes unity.

($\mu^+\text{SR}$), where a vortex state is induced in an applied magnetic field and the time t dependence of muon-spin polarization is fitted with a Gaussian model, $\exp(-\sigma_\mu^2 t^2/2)$. Results for σ_μ/γ_μ , where $\gamma_\mu = 8.514 \times 10^5 \text{ G}^{-1}\text{s}^{-1}$ is the muon gyromagnetic ratio, provide estimates of the superconducting magnetic penetration depth λ through the theoretical relation, $\sigma_\mu/\gamma_\mu = (1.26 \times 10^{-8} \text{ G cm}^2) \lambda^{-2}$, where for ceramic specimens of $(\text{Ca}_x\text{La}_{1-x})(\text{Ba}_{1.75-x}\text{La}_{0.25+x})\text{Cu}_3\text{O}_y$, as well as $\text{YBa}_2\text{Cu}_3\text{O}_{7-\delta}$, λ^{-2} is obtained as a crystallographic average dominated by the basal (a - b) plane component.¹⁴⁻¹⁶ Under optimal experimental and materials conditions, which require a nearly perfectly formed and static lattice of fluxons within a homogeneous clean superconducting material,¹⁷ the zero-temperature limit, denoted as $\lambda(0)$, yields the London penetration depth $\lambda_L = (m^*c^2/4\pi n_S e^2)^{1/2}$, reflecting the intrinsic superconducting carrier density n_S and an effective mass m^* .¹⁸ On the other hand, the presence of disorder and inhomogeneity introduces residual normal conductivity that increases the measured $\lambda(0)$ relative to the intrinsic penetration depth (discussed, e.g., in Ref. 19).

In superconducting material of high quality, the residual mean-free path $\ell_{\text{mfp}}(0)$ is generally larger than the Pippard coherence distance ξ_0 , obeying a criterion that is equivalent to $\hbar\tau^{-1}(0)/k_B T_C < 1$, where $\tau^{-1}(0)$ is the residual scattering rate (\hbar is reduced Planck's constant; k_B is the Boltzmann constant). It is useful to estimate $\tau^{-1}(0)$ from $\lambda(0)$ and the extrapolated residual resistivity $\rho(0) = m^*\tau^{-1}(0)/ne^2$, where n is the normal-state carrier density, by equating the normal m^*/n to the superconducting m^*/n_S . The result, $\tau^{-1}(0) = 4\pi c^{-2}\lambda^{-2}(0)\rho(0)$, has been evaluated using measurements of σ_μ from Ref. 6. The ratio $\hbar\tau^{-1}(0)/k_B T_C$ is plotted in the inset of Fig. 2, where the horizontal dashed line denotes unity. Points falling above the dashed line indicate low quality for specimens with $x < 0.4$. One notes that this measure of quality is obtained more accurately at low x , where $\rho(0)$ becomes comparable to $\rho(T_C^+)$ [see Fig. 2]; moreover, $\lambda^{-2}(0)$ determined from σ_μ is an upper bound at low x , since it is uncorrected for disorder.¹⁹

Figures 1 and 2, which represent data corresponding to the highest T_C for a given x , are consistent with identifying a unique T_C^{\max} for the optimum transition temperature of $(\text{Ca}_x\text{La}_{1-x})(\text{Ba}_{1.75-x}\text{La}_{0.25+x})\text{Cu}_3\text{O}_y$, validating the conclusions drawn in Ref. 2, which were deduced by scaling methodologies involving x , y , and c . Alternative interpretations have been derived from variations in

superconducting and magnetic properties with x - y stoichiometry²⁰⁻²² and are discussed in Sec. IV.

Values of T_C and σ_μ (low-temperature limit) from μ^+ SR measurements of $(\text{Ca}_x\text{La}_{1-x})(\text{Ba}_{1.75-x}\text{La}_{0.25+x})\text{Cu}_3\text{O}_y$ samples with various x and y were previously presented in Ref. 6, including some sketches to suggest curved or looped trends. The data corresponding to $x = 0.4$ are represented in Fig. 3 as filled circles (underdoped with respect to optimum y) and filled triangles (overdoped with respect to optimum y). Data corresponding to the highest T_C for $x = 0.1$ and $x = 0.4$ are represented by the filled squares and distinguished by the arrows. As noted in Ref. 6, variations of T_C with σ_μ tend to be insensitive to whether materials are underdoped or overdoped. In particular, the datum for $x = 0.1$ is observed to commingle with data for non-optimal samples, e.g., the filled square is adjacent to a filled circle (data for $x = 0.2$ and $x = 0.3$ in Ref. 6 display the same type of behavior).

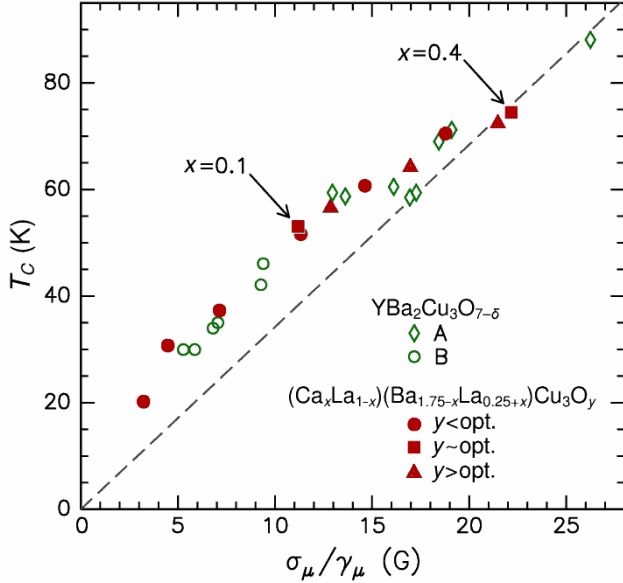


FIG. 3. Transition temperature measured by μ^+ SR plotted against the μ^+ SR Gaussian relaxation parameter divided by the muon gyromagnetic ratio, σ_μ/γ_μ , for polycrystalline samples of $(\text{Ca}_x\text{La}_{1-x})(\text{Ba}_{1.75-x}\text{La}_{0.25+x})\text{Cu}_3\text{O}_y$ with depleted oxygen at $x = 0.4$ (filled circles), excess oxygen at $x = 0.4$ (filled triangles), and optimum oxygen at $x = 0.1$ and $x = 0.4$ (filled squares, distinguished by arrows) after Ref. 6. Similarly obtained μ^+ SR data for ceramic samples of $\text{YBa}_2\text{Cu}_3\text{O}_{7-\delta}$ for various δ are presented for comparison; A (open diamonds) after Ref. 23 and B (open circles) after Ref. 24. Dashed line is reproduced from Ref. 26.

For comparison, Fig. 3 includes similarly obtained μ^+ SR data for $\text{YBa}_2\text{Cu}_3\text{O}_{7-\delta}$ (open diamonds represent data set A from Ref. 23; open circles represent data set B from Ref. 24). For $\text{YBa}_2\text{Cu}_3\text{O}_{7-\delta}$ the variation of T_C in this case is induced solely by oxygen depletion, which has the notable propensity of creating percolative superconductivity (e.g., as observed in recent heat capacity studies²⁵). The dashed line in Fig. 3, which has been used to reference μ^+ SR data in several previous publications (e.g., Refs. 6 and 26–28), is discussed in Sec. IV. In the case of $\text{YBa}_2\text{Cu}_3\text{O}_{7-\delta}$, many of the data points fall to the left of the dashed line, which represent depressed σ_μ for a given T_C ; this corresponds to $\lambda > \lambda_L$ and is consistent with non-optimal superconducting samples. The notable exception is the ortho-II phase $\text{YBa}_2\text{Cu}_3\text{O}_{6.60}$ containing ordered chain oxygens; the point for this optimum 60-K superconductor is near the dashed line. It is quite evident that much of the data for $(\text{Ca}_x\text{La}_{1-x})(\text{Ba}_{1.75-x}\text{La}_{0.25+x})\text{Cu}_3\text{O}_y$ display a pattern of overlapping the results for these nonoptimal $\text{YBa}_2\text{Cu}_3\text{O}_{7-\delta}$ materials, especially in the region $T_C < 60$ K. The possible exception is the $x = 0.4$ sample with highest T_C and σ_μ , and indicated by a filled square in Fig. 3; for this sample, both x and y appear to be closest to optimum. This μ^+ SR result is also consistent with evidence from resistivity and susceptibility that optimal $(\text{Ca}_x\text{La}_{1-x})(\text{Ba}_{1.75-x}\text{La}_{0.25+x})\text{Cu}_3\text{O}_y$ corresponds to x of at least 0.4.

Other important results have been reported,²⁹ where integrated XAS of the Cu_{2p} L_3 edge and O_{1s} K edge of $(\text{Ca}_x\text{La}_{1-x})(\text{Ba}_{1.75-x}\text{La}_{0.25+x})\text{Cu}_3\text{O}_y$ each reveal very weak variation with x at optimum y (less than one standard deviation and about two standard deviations, respectively, for a 0.4-change in x), interpreted in Ref. 29 as near invariance of the charge per planar Cu and O with x . Conversely, Cu_{2p} L_3 and O_{1s} K XAS do detect the expected change in charge on both Cu and O with variation of y at constant x , confirming that XAS is indeed sensitive to carrier density variations associated with the cuprate-planes. The charge invariance of the planar Cu and O ions with x provides an independent rationale for grouping together the varied stoichiometries of $(\text{Ca}_x\text{La}_{1-x})(\text{Ba}_{1.75-x}\text{La}_{0.25+x})\text{Cu}_3\text{O}_y$, such as the various x at local optimum y presented in Figs. 1 and 2.

Independence of the carrier density in the cuprate planes for variable x and constant y may be understood in terms of charge compensation doping in $(\text{Ca}_x\text{La}_{1-x})(\text{Ba}_{1.75-x}\text{La}_{0.25+x})\text{Cu}_3\text{O}_y$. Consider the layers adjacent to the cuprate planes from the perspective of charge

balance. The cation charge state in the $\text{Ba}_{1.75-x}\text{La}_{0.25+x}\text{O}_2$ layers increases as $x/2$ per layer; the cation charge state in the $\text{Ca}_x\text{La}_{1-x}$ layer decreases by x , which is a decrease of $x/2$ per cuprate plane; hence, the sum of the charges on the cations in the two layers adjacent to a given cuprate plane remains constant with x .

III. THEORETICAL FORMULATION

The theoretical model of Ref. 5 of the pairing mechanism governing high- T_C superconductivity assumes that the pairing interaction occurs between physically separated carrier bands via Coulomb interactions. In the case of $\text{YBa}_2\text{Cu}_3\text{O}_{7-\delta}$, for example, the interacting charges are located in adjacent BaO and CuO_2 layers, separated perpendicularly by an interaction distance ζ , with the former designated as part of the type I reservoir (i.e., BaO-CuO-BaO) and the latter assigned to the type II reservoir (i.e., CuO_2 -Y-CuO₂). Here, the CuO and Y layers are referred to as central doping (or inner) layers and the BaO and CuO_2 layers as interacting (or outer) layers. Defining ℓ to be the mean in-plane spacing between interacting charges, the optimal transition temperature T_{C0} , corresponding to the highest T_C for a given compound structure and doping, is given by the algebraic equation,

$$T_{C0} = k_B^{-1} \beta / \ell \zeta = k_B^{-1} \beta (\sigma \eta / A)^{1/2} / \zeta, \quad (1)$$

where η is the number of charge-carrying layers in the type II reservoir (e.g., $\eta = 2$ for $\text{YBa}_2\text{Cu}_3\text{O}_{7-\delta}$ and $(\text{Ca}_x\text{La}_{1-x})(\text{Ba}_{1.75-x}\text{La}_{0.25+x})\text{Cu}_3\text{O}_y$, corresponding to the two CuO_2 planes), σ is the fractional charge per outer type I layer per formula unit for participating carriers, A is the basal-plane area per formula unit, $\ell = (\sigma \eta / A)^{-1/2}$, and $\beta (= 0.1075 \pm 0.0003 \text{ eV } \text{Å}^2)$ is a universal constant, where β/e^2 has dimensions of length (0.00747 Å) and is equal to about twice the reduced electron Compton wavelength. The optimization of the superconducting state is achieved when the interacting carrier densities associated with the type I and type II reservoirs are in equilibrium, with superconductivity in these systems occurring for $\zeta/\ell \leq 1$.⁵

A. Application of Eq. (1)

In general, doping may be either cation or anion and can occur in either reservoir⁵ or in both. For compounds (such as $\text{La}_{1.837}\text{Sr}_{0.163}\text{CuO}_4$) where the doping is clearly known, σ can be determined directly by allocating the doping charge to the structural layers

and charge reservoirs through application of (a first set of) rules (1a) and (1b) that are discussed in Refs. 5 and 12. However, for those compounds in which the doping charge cannot be discerned independently, e.g., $\text{BiSr}_2\text{CaCu}_2\text{O}_{8+\delta}$, σ can be calculated by scaling to $\sigma_0 (= 0.228)$ for $\text{YBa}_2\text{Cu}_3\text{O}_{6.92}$ according to the formula,

$$\sigma = \gamma \sigma_0, \quad (2)$$

where γ is the product of individual scaling factors γ_i , which are all dependent upon structure and/or charge state. Since one is primarily interested in determining the charge in the type I interacting layers, γ is by default equal to γ_1 (i.e., the scaling factor corresponding to the type I reservoir). The following (second set of) valency scaling rules are used to determine the γ_i comprising γ in Eq. (2).

(2a) Heterovalent substitution [in the type I central layer(s)] of a valence +3 ion mapped to a valence +2 ion corresponding to the $\text{YBa}_2\text{Cu}_3\text{O}_{7-\delta}$ structural type introduces a factor of 1/2 in γ .

(2b) The factor γ scales with the +2 (−2) cation (anion) structural and charge stoichiometry associated with participating charge.

(2c) The factor γ scales with the net valence of the undoped mediating layer.

Note that the first two valence scaling rules above are defined to be applicable to the type I reservoirs of the cuprate-plane containing superconductors (doping is typically introduced by cation substitution in the type I reservoirs).³⁰ For example, rule (2b) requires scaling the +2 ion content (as applied to the outer layers) or the number of layers [applied, e.g., to the central donor layer(s) of $\text{Bi}_2\text{Sr}_2\text{CaCu}_2\text{O}_{8+\delta}$ (Ref. 5)] to that of $\text{YBa}_2\text{Cu}_3\text{O}_{6.92}$. For the particular case of $(\text{Ca}_x\text{La}_{1-x})(\text{Ba}_{1.75-x}\text{La}_{0.25+x})\text{Cu}_3\text{O}_y$, only rule (2b) is used with specific regard to the relative Ba^{+2} content.

B. Calculation of T_{C0}

From Fig. 1, the maximum transition temperature for $(\text{Ca}_x\text{La}_{1-x})(\text{Ba}_{1.75-x}\text{La}_{0.25+x})\text{Cu}_3\text{O}_y$ occurs for $0.4 \leq x \leq 0.5$, with a value ranging between 77.8 – 79.2 K from (onset) susceptibility, and 79.3 – 80.6 K from resistivity, obtained by taking onset values minus the transition widths; samples for these data correspond to $y = 7.135 - 7.141$.¹ For the mid-range point, $x = 0.45$ and $y = 7.135$, the resistive zero occurs at $T_C^{\text{max}} = 80.5$ K, which for the purposes of this paper will be taken to be the experimentally measured T_{C0} (this stoichiometry also produces the sharpest magnetic transition¹).

Determining σ , corresponding to the optimal compound of this series, is accomplished by utilizing the valence scaling rule (2b) for the type I outer layers. Application of this rule requires scaling the outer layer Ba^{+2} content of $1.75 - x$ in $(\text{Ca}_x\text{La}_{1-x})(\text{Ba}_{1.75-x}\text{La}_{0.25+x})\text{Cu}_3\text{O}_y$ with respect to the two Ba^{+2} ions in stoichiometric $\text{YBa}_2\text{Cu}_3\text{O}_{6.92}$. Thus γ is given by $(1.75 - x)/2$, such that one then has from Eq. (2),

$$\sigma = \gamma \sigma_0 = [(1.75 - x)/2] \sigma_0. \quad (3)$$

The value of x in Eq. (3) corresponds to the optimal superconducting state, and has been determined by the examination of experimental data in Sec. II to be approximately 0.45. Unfortunately, structural data for $x = 0.45$ are not available, so T_{C0} is calculated for both $x = 0.4$ and 0.5 using structural data from x-ray diffraction for sintered and oxygenated samples in Ref. 1. For $x = 0.40$, $A = a^2 = (3.876 \text{ \AA})^2 = 15.0234 \text{ \AA}^2$ and $\zeta = 2.1593 \text{ \AA}$, where a is the basal lattice parameter and ζ is the difference in z heights between the Ba(La) and O(2)-plane sites.⁵ Given $\sigma = \gamma \sigma_0 = [(1.75 - 0.40)/2] 0.228 = 0.1539$, one obtains $\ell = (A/\sigma\eta)^{1/2} = 6.9863 \text{ \AA}$, $(\ell\zeta)^{-1} = 0.06629 \text{ \AA}^{-2}$, and Eq. (1)

yields $T_{C0} = 82.69 \text{ K}$. Notice that the calculated $\sigma = 0.1539$ is nearly the same as the cuprate-plane holes $n_p = 0.16 \pm 0.02$ for optimum oxygen obtained in Ref. 29. Similarly for $x = 0.50$, $A = (3.873 \text{ \AA})^2 = 15.0001 \text{ \AA}^2$, $\zeta = 2.1001 \text{ \AA}$, $\sigma = 0.1425$, $\ell = 7.2548 \text{ \AA}$, $(\ell\zeta)^{-1} = 0.06564 \text{ \AA}^{-2}$, and $T_{C0} = 81.88 \text{ K}$. Since T_C is rather independent of x in this regime,⁶ one can write a calculated average of $\langle(\ell\zeta)^{-1}\rangle = 0.06597 \text{ \AA}^{-2}$ (i.e., $\langle\ell\rangle = 7.1206 \text{ \AA}$ and $\langle\zeta\rangle = 2.1297 \text{ \AA}$), corresponding to $\langle T_{C0}\rangle = 82.29 \text{ K}$, which is adopted for the theoretical result. Given the uncertainties in the Rietveld refinements and the range in x , the estimated error in $\langle T_{C0}\rangle$ is $\pm 0.44 \text{ K}$; rounding to one significant decimal digit, $\langle T_{C0}\rangle = 82.3(4) \text{ K}$. This result for T_{C0} is plotted at $x = 0.45$ in Fig. 1 and compared to T_C values extracted from resistivity and susceptibility data.^{1,2,4}

It is important to note that T_C of $(\text{Ca}_x\text{La}_{1-x})(\text{Ba}_{1.75-x}\text{La}_{0.25+x})\text{Cu}_3\text{O}_y$ appears to increase slightly under hydrostatic pressure (see inset of Fig. 1).² Although the data set is rather limited (data only available for pressures $\leq 0.8 \text{ GPa}$), dT_C/dP decreases rapidly as x approaches $0.4 - 0.5$ from below, indicative of optimization at or near ambient pressure.

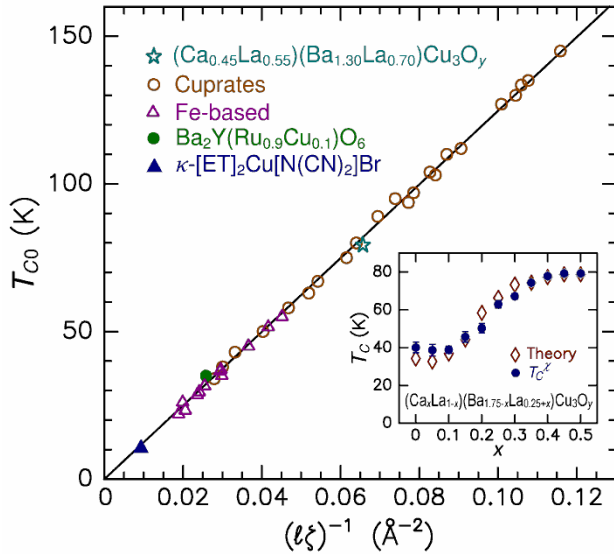


FIG. 4. Experimental T_{C0} vs $(\ell\zeta)^{-1}$, where ℓ is intra-layer mean spacing of interacting charges and ζ is inter-layer interaction distance, for $(\text{Ca}_{0.45}\text{La}_{0.55})(\text{Ba}_{1.30}\text{La}_{0.70})\text{Cu}_3\text{O}_y$ ($x = 0.45$, star symbol), compared to other cuprates (open circles), Fe-based pnictides and chalcogenides (open triangles), a ruthenate (filled circle) and an organic (filled triangle). The solid line through the data points represents Eq. (1). Inset: transition temperatures T_C^x of $(\text{Ca}_x\text{La}_{1-x})(\text{Ba}_{1.75-x}\text{La}_{0.25+x})\text{Cu}_3\text{O}_y$ (filled symbols) and pair-breaking theory [Eq. (4), open symbols] as a function of doping x .

Figure 4 shows the experimentally determined values of T_{C0} plotted against the respective calculated values of $(\ell\zeta)^{-1}$ for $(\text{Ca}_x\text{La}_{1-x})(\text{Ba}_{1.75-x}\text{La}_{0.25+x})\text{Cu}_3\text{O}_y$ (star symbol, for an average $x = 0.45$), compared to other cuprates (open circles), Fe-based pnictides and chalcogenides (open triangles), a ruthenate (filled circle), and an organic (filled triangle). The solid line through the data points, totaling 37 compounds, represents Eq. (1) with $k_B^{-1}\beta = 1247.4 \text{ K}\cdot\text{\AA}^2$ unchanged from the original publication,⁵ successfully and accurately predicting T_{C0} to within $\pm 1.35 \text{ K}$ (fitting β anew yields statistically unchanged results: $k_B^{-1}\beta = 1246.0 \pm 3.6 \text{ K}\cdot\text{\AA}^2$ and same accuracy in T_{C0}).³¹

C. Variation of T_C with x

A plausible implication of relatively high residual scattering found at low x , particularly for $x = 0.1$, is that T_C is depressed by pair-breaking effects. In the presence of a spin-flip scattering rate τ_p^{-1} , the pair-breaking effect yields a transition temperature T_C that is reduced relative to the optimum T_{C0} , and is obtained theoretically from the expression,

$$\ln(T_{C0}/T_C) = \psi(1/2) - \psi(1/2 + \hbar\tau_p^{-1}/4\pi k_B T_C), \quad (4)$$

where ψ is the digamma function (see, e.g., Refs. 11 and 32). In the application of this theory in Ref. 32 to

$\text{YBa}_2\text{Cu}_3\text{O}_{7-\delta}$ modified by atomic substitutions, τ_p^{-1} was taken to scale with an assumed concentration of magnetic impurities; it is further shown in Ref. 11 that disorder, such as the kind produced by doping $\text{YBa}_2\text{Cu}_3\text{O}_{7-\delta}$ with Pr on Ba sites, yields a variation in T_C in accordance with Eq. (4).

Pair-breaking theory is compared with experiment in the inset of Fig. 4. Filled symbols denote data at various x for T_C^x determined from magnetic susceptibility (error bars are $\Delta T_C/2$). The open symbols are theoretical T_C from Eq. (4), calculated by modeling the pair-breaking rate as a fraction \tilde{a} of the residual scattering rate and expressed as $\tau_p^{-1} = \tilde{a} \tau^{-1}(0)$, where \tilde{a} is an empirical constant and $\tau^{-1}(0)$ is determined from data for the residual resistivity and muon-spin depolarization (interpolation and extension of x dependence was used to determine $\rho(0)$ and σ_μ for which data are unavailable). The fit of Eq. (4) to T_C^x yields $T_{C0} = 81.1$ K, $\tilde{a} = 0.24$, and fitting accuracy of 2 K; uncertainty in each parameter is at least 0.5%, as estimated from ΔT_C and exclusive of other experimental uncertainties (e.g., the systematic error in σ_μ). Therefore, the hypothesis of a single optimum parent composition, which becomes non-optimum at reduced x owing to the effects of pair breaking disorder, is consistent with the data on $(\text{Ca}_x\text{La}_{1-x})(\text{Ba}_{1.75-x}\text{La}_{0.25+x})\text{Cu}_3\text{O}_y$. While magnetic impurities have not been reported for the various x at optimum y , the spin-flip scattering may be connected to local moment formation in superconducting material with underdoped y .²⁰

IV. DISCUSSION

The new datum for $(\text{Ca}_{0.45}\text{La}_{0.55})(\text{Ba}_{1.30}\text{La}_{0.70})\text{Cu}_3\text{O}_y$ included in Fig. 4 provides additional support for the universality of the high- T_C model described herein and elsewhere.^{5,12,13} The adherence of this unique charge-compensated compound to Eq. (1) also confirms that inhomogeneity and magnetism are incompatible with optimal high- T_C superconductivity. Based on interlayer Coulomb coupling, and recognizing that measurements made only on optimal materials will necessarily reflect the intrinsic superconducting state, this theory has been shown to be valid for 37 different optimal compounds representing six superconducting families. As described in Sec. III, the interacting charge density ℓ^{-2} follows from the charge fraction σ that, in itself, is not a universal constant among the various optimal cuprate compounds [Eq. (2)]. This stands in stark contrast with earlier models representing T_C as a function

solely of a doping parameter,^{33,34} which do not distinguish the carriers actually participating in the pairing interaction. Such models were recently applied to $(\text{Ca}_x\text{La}_{1-x})(\text{Ba}_{1.75-x}\text{La}_{0.25+x})\text{Cu}_3\text{O}_y$ for the purposes of XAS calibration²⁹ and for asserting inconsistency.³⁵ Another significant deficiency in models restricted to doping dependence (e.g., as in Ref. 36 for $\text{YBa}_2\text{Cu}_3\text{O}_{7-\delta}$) is the omission of the interaction distance ζ ; inclusion of this structural length in Eq. (1) proves to be essential for universal accuracy in predicting T_C , given that high- T_C superconductivity originates from interlayer Coulomb interactions.

While the negligible XAS spectral response with x observed for the planar Cu and O ions²⁹ is seemingly in conflict with transport and susceptibility measurements showing a significant correlation of T_C with x (Fig. 1), and $\mu^+\text{SR}$ experiments finding significant variation of σ_μ with x (e.g., the two square data points of Fig. 3 and in Ref. 6), it does indicate that the variation of T_C with cation substitution^{6,20-22,35} is unrelated to the two-dimensional (2D) carrier density in the cuprate planes.³⁷ Implicit in this dichotomy is that $\mu^+\text{SR}$ measurements (and other techniques) are insensitive in probing superconductivity associated with the CuO_2 planes. Taken together, these studies therefore locate the superconducting hole condensate in the type I reservoirs (La-substituted BaO-CuO-BaO structures). Experimental uncertainty in XAS allows only for a possible 12% of the superconducting fraction to reside in the cuprate layers.

In much of the previously published work on $\text{Ca}_x\text{La}_{1-x})(\text{Ba}_{1.75-x}\text{La}_{0.25+x})\text{Cu}_3\text{O}_y$ it was assumed that the doping (both x and y) can be varied rather widely without affecting the quality of the superconducting condensate. Each value of x was assumed to constitute a different cuprate family, owing to variations in structure (lattice parameters and oxygen buckling angles)²¹ and critical doping levels.²² Such a designation assumes equal significance among the local maxima in T_C associated with each x , which is incommensurate with the experimental evidence for degradation of the superconducting condensate for $x < 0.4$ (for any given value of y), exhibited, e.g., by the corresponding resistivities, susceptibilities, transition widths, and residual carrier scattering. From Figs. 1 and 2, it is evident that there exists only one unique optimal stoichiometry, which is achieved for x between 0.4 and 0.5.

The initial offset introduced by the substitution of 12.5% La^{+3} into the Ba^{+2}O layers of the parent

compound $\text{LaBa}_2\text{Cu}_3\text{O}_{7-\delta}$ reduces the charge available for superconductivity, thereby limiting the ultimate value of T_{C0} achievable. The initial imbalance of charge introduced between the type I and type II reservoirs is clearly observed from the pressure dependence (see inset of Fig. 1), which shows a decreasing dT_C/dP as x approaches 0.4 from below. Application of hydrostatic pressure facilitates charge transfer along the hard axis; the structurally related compound, $\text{YBa}_2\text{Cu}_4\text{O}_8$, is a good example of the effect of pressure in optimizing T_C .³⁸ The fact that dT_C/dP approaches zero for $x \sim 0.4$ indicates an ambient-pressure charge equilibrium corresponding to the one optimal stoichiometry.

A. Trends in optimal oxygen doping

Obtaining the charge fraction σ by scaling to σ_0 of the optimal compound $\text{YBa}_2\text{Cu}_3\text{O}_{6.92}$ is predicated on implicit optimization of the oxygen stoichiometry in the high- T_C cuprates under consideration. Figure 5 examines this by plotting the oxygen content y against T_C for two parent compounds of $(\text{Ca}_x\text{La}_{1-x})(\text{Ba}_{1.75-x}\text{La}_{0.25+x})\text{Cu}_3\text{O}_y$, namely $\text{LaBa}_2\text{Cu}_3\text{O}_y$ [$T_{C0} = 97$ K from Ref. 39 (y not given), $y = 6.85$ from Ref. 40, filled square⁴¹] and $\text{YBa}_2\text{Cu}_3\text{O}_y$ ($T_{C0} = 93.78$ K, $y = 6.92$ from Ref. 42, filled triangle), corresponding to

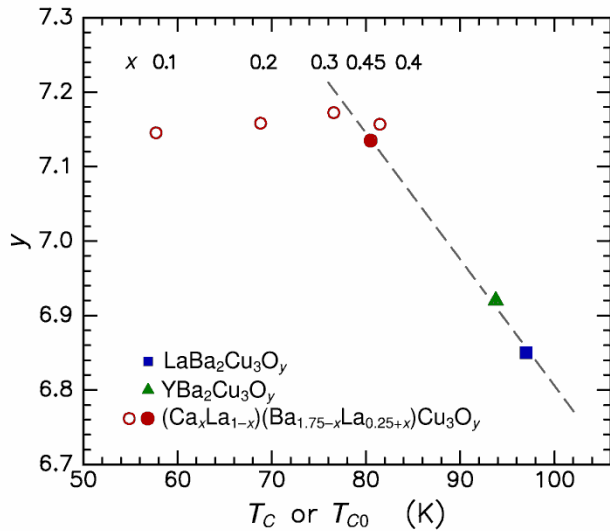


FIG. 5. Variation of oxygen parameters y with transition temperatures for $\text{LaBa}_2\text{Cu}_3\text{O}_y$ and $\text{YBa}_2\text{Cu}_3\text{O}_y$ (filled symbols, T_{C0} at optimum y), and for $(\text{Ca}_x\text{La}_{1-x})(\text{Ba}_{1.75-x}\text{La}_{0.25+x})\text{Cu}_3\text{O}_y$ from resistive onset T_C at $x = 0.1$, 0.2 , 0.3 , and 0.4 after Ref. 4, open circles, and experimental optimum T_{C0} at $x = 0.45$ (see Sec. III B), filled circle. Dashed line denotes linear fit to the optimum compounds.

optimum y for each, and for $(\text{Ca}_x\text{La}_{1-x})(\text{Ba}_{1.75-x}\text{La}_{0.25+x})\text{Cu}_3\text{O}_y$, where y corresponds to highest (resistive onset) T_C values of 57.7, 68.8, 76.6, and 81.5 K for $x = 0.1$, 0.2 , 0.3 , and 0.4 , respectively (open circles).⁴ The filled circle corresponds to $x = 0.45$, $y = 7.135$ and $T_{C0} = 80.5$ K, as determined for optimal $(\text{Ca}_x\text{La}_{1-x})(\text{Ba}_{1.75-x}\text{La}_{0.25+x})\text{Cu}_3\text{O}_y$ in Sec. III B from data in Ref. 1. A dashed line is fitted to the data for the three optimum compounds (filled symbols), indicating the linear trend [slope $-0.017(9) \text{ K}^{-1}$, intercept $8.50(8)$, linear correlation coefficient $R^2 = 0.997$, and fitting error $\delta y = 0.011$]. Three open circle symbols corresponding to $(\text{Ca}_x\text{La}_{1-x})(\text{Ba}_{1.75-x}\text{La}_{0.25+x})\text{Cu}_3\text{O}_y$ with non-optimum doping ($x < 0.4$) deviate to the left of this trend line. Of particular interest is that the 40% variation in T_C with x is associated with rather small changes in y , i.e., the trend in $(\text{Ca}_x\text{La}_{1-x})(\text{Ba}_{1.75-x}\text{La}_{0.25+x})\text{Cu}_3\text{O}_y$ is very much weaker than expected for a series of optimum compounds (dashed line). Near invariance of y suggests that the charge balance between the two reservoir types changes with the charge compensation variable x , which is non-optimum for $x < 0.4$, where depressed and broadened transitions are observed (Figs. 1 and 2).

Combining the various reported results for optimal superconductivity in $(\text{Ca}_x\text{La}_{1-x})(\text{Ba}_{1.75-x}\text{La}_{0.25+x})\text{Cu}_3\text{O}_y$, the optimal oxygen content is estimated as $y_0 = 7.15 \pm 0.02$, the optimal charge compensation variable is in the range $0.4 \leq x \leq 0.5$, and the unique optimal T_{C0} , determined by various methodologies, is in the range 80.5 to 82 K.^{1-4,21,29,35}

For the oxygen underdoped compositions, the onset of superconductivity occurs in the vicinity of a threshold y_c that systematically decreases with increasing x . According to Fig. 1 of Ref. 20, $y_c \approx 6.97$ at $x = 0.1$ and $y_c \approx 6.88$ at $x = 0.4$. Since superconductivity is already degraded at $x = 0.1$ (e.g., insets in Figs. 2 and 4), it is logical that less relative oxygen doping $(y_0 - y_c) = 0.17$ (compared to 0.27 at $x = 0.4$) is sufficient for destroying superconductivity. However, one recognizes that alternative interpretations of the x - y behavior have proposed various x -dependent factors to scale the y dependence.^{2,6,20-22,35} In one of these, comparing ¹⁷O NQR data at $x = 0.1$ and 0.4 , variations in superconductivity and magnetism are attributed to an x dependence in the efficiency of hole injection.²² Remaining unaccounted for by various x -dependent scaling methods are the O_{1s} K -edge XAS measurements that find no x dependence in the carrier concentration at the cuprate-plane O site.²⁹ A plausible explanation is that degradation of the Ca/La

and Ba/La stoichiometries tends to be compensated by adjustments in $(y_0 - y_c)$. Experimental results, particularly the near invariance of y_0 , therefore validate the unique value for T_{C0} , which is used in the analysis of T_C according to Eq. (4).

B. Inhomogeneous superconductors

Superconducting transition temperatures measured as a function of doping typically exhibit a “superconducting dome” effect (a rise in T_C followed by a fall, as stoichiometry passes through the underdoped-optimal-overdoped regimes); this same behavior was found in $(\text{Ca}_x\text{La}_{1-x})(\text{Ba}_{1.75-x}\text{La}_{0.25+x})\text{Cu}_3\text{O}_y$ by the non-monotonic variation of T_C with y at constant x .^{4,21} Figure 1 illustrates that T_C also arches over to a maximum as a function of x (at optimum y), accompanied by a sharpening of the superconducting transition; the region $x < 0.4$ therefore exhibits the hall marks of percolative inhomogeneous superconductivity in the underdoped regime (see, e.g., Ref. 43; formulations with $x \geq 0.6$ turn out to yield phase-separated samples¹).

The $\mu^+\text{SR}$ data of Fig. 3 suggest a similar tendency for T_C to approach a maximum as a function of σ_μ/γ_μ . For underdoped cuprates the variation of T_C with σ_μ is of interest in connection with the pseudogap phenomenon, identified by a characteristic temperature $T^* > T_C$.^{19,43-45} For example, a resonating valence bond model applied to calculating the penetration depth has found that the “dome” characteristic of T_C vs doping translates into a similar non-linear dependence of T_C on $\lambda^{-2}(0)$ that has been favorably scaled to experimental data on selected compounds.⁴⁵

The dashed line of Fig. 3 has been considered in terms of a granular texture model of inhomogeneous superconductivity from which a similar proportionality between T_C and $\lambda^{-2}(0)$ has been derived theoretically (coefficient reproduced to within a factor of 2).⁴⁶ In a compendium of experimental data that includes nonoptimum compounds, it was found that T_C multiplied by the normal-state conductivity is proportional to $\lambda^{-2}(0)$ with about $\pm 20\%$ error; this correlation is attributed to the influence of disorder scattering.⁴⁷ Universal proportionality between T_C and σ_μ , or the amended nearly linear scaling discussed in Ref. 27, are at best qualitative concepts¹⁹ that were shown to be in disagreement with $\mu^+\text{SR}$ data.⁴⁸ Moreover, the relation $\sigma_\mu \propto n_s/m^*$ can only be considered an idealization, uncorrected for perturbations by materials inhomogeneity, electronic disorder and

fluxon pinning effects (see, e.g., Ref. 16). This is clearly demonstrated in Fig. 3 in the case of $(\text{Ca}_x\text{La}_{1-x})(\text{Ba}_{1.75-x}\text{La}_{0.25+x})\text{Cu}_3\text{O}_y$,⁴⁹ and also by the data for $\text{YBa}_2\text{Cu}_3\text{O}_{7-\delta}$,²³ where T_C for samples near the optimum 90-K phase varies by 1.2% (91.3 to 92.4 K), yet results for σ_μ vary by 40 %, corresponding to a factor of 1.5, with most of these data falling to the right of the (extrapolated) dashed line of Fig. 3.

Specific evidence that $x = 0.1$ tends to form inhomogeneous material is found in resistivity and magnetization data on $(\text{Ca}_x\text{La}_{1-x})(\text{Ba}_{1.75-x}\text{La}_{0.25+x})\text{Cu}_3\text{O}_y$ single crystals grown with optimum y .⁵⁰ In Fig. 3 of Ref. 50, an $x = 0.1$ crystal exhibits a very broad transition, extending from an onset near 79 K to full superconductivity below 50 K, clearly reflecting an inhomogeneous superconducting state. A similarly prepared crystal with $x = 0.4$ exhibits sharp resistive and magnetic transitions with an onset near 81 K, consistent with results for ceramic specimens. Another anomaly associated with $x = 0.1$ is the absence of a metallic transport at overdoping in y where $T_C = 0$, as revealed by a minimum in the temperature dependence of $\rho(T)$.⁵¹ Interpreted as absence of a quantum critical point in y ,⁵¹ this finding makes it difficult to treat formulations with $x = 0.1$ as a separate family of $(\text{Ca}_x\text{La}_{1-x})(\text{Ba}_{1.75-x}\text{La}_{0.25+x})\text{Cu}_3\text{O}_y$ compounds. The broadened transitions also create difficulties in quantifying a superconducting dome (T_C vs y); for example, at $x = 0.1$ and $y = 6.986$, which is underdoped and above the minimum for superconductivity, the claimed T_C value of about 16 K entered in the phase diagram corresponds to a specimen that is non-superconducting above 5 K and has a negative resistivity slope between 25 and 80 K (see Fig. 6 of Ref. 4).⁴

C. Superconductivity and magnetism in $(\text{Ca}_x\text{La}_{1-x})(\text{Ba}_{1.75-x}\text{La}_{0.25+x})\text{Cu}_3\text{O}_y$

In a series of presentations of experimental studies, the superconductivity was related to magnetism in underdoped $(\text{Ca}_x\text{La}_{1-x})(\text{Ba}_{1.75-x}\text{La}_{0.25+x})\text{Cu}_3\text{O}_y$, through various constructions of reduced phase diagrams, where changes in y were scaled by factors varying with x .^{20,22,35,52} The differing approaches (e.g., Refs. 20 and 22) show the commonality in how magnetism becomes disordered and diminishes, concomitant with the emergence of superconductivity, as y is increased from 6.4 to 7.15 (a difference of 0.75). Part of that commonality is exhibited by the variation of Néel temperature T_N with x and y , where an x -independent crossing (or stationary) point occurs at $y \sim 6.5$ and $T_N \approx 380$ K. Although T_N is defined by a

sharp phase transition at extreme oxygen depletion ($y \sim 6.4$), significant broadening becomes evident for y near the spin-glass region (e.g., $T_N = 221$ K of width > 35 K for $x = 0.1$, $y = 6.858$, and where $T_C = 0$),²⁰ indicating that phase diagram analysis encompasses materials with inhomogeneous magnetism. Evidently, the values y_N constructed in Ref. 20 from y dependence in T_N connote the onsets of inhomogeneity in antiferromagnetic ordering, which is consistent with the generally inhomogeneous spin-glass freezing.^{20,52} Since phase separation is not expected to broaden T_N , critical oxygen levels such as y_N point to intrinsic magnetic inhomogeneity,⁵² rather than a possibility of phase transitions,²² analogous to how y_c is related to the destruction of superconductivity in the presence of magnetism.

The μ^+ SR measurements of superconducting and spin-glass properties of y -underdoped $(\text{Ca}_x\text{La}_{1-x})(\text{Ba}_{1.75-x}\text{La}_{0.25+x})\text{Cu}_3\text{O}_y$, particularly in the region where the two phases coexist, had earlier prompted the suggestion of microscopic phase separation.⁵² In a later study using ^{63}Cu NQR, a possibility of mesoscopic inhomogeneities remained.³⁵ However, a more recent work, which included comparisons of ^{17}O NQR at $x = 0.1$ and 0.4 , has posited changes in oxygen doping efficiency.²² Generally shown in these studies is that underdoping in x allows for less underdoping in y , i.e., underdoping in both x and y depletes carriers synergistically. The most notable feature common to all of the various scaled phase diagrams constructed from these observations^{20,22,35,52} is the nearly x -independent oxygen doping at highest T_C , which is consistent with a unique optimal superconducting composition, and in contrast to the shifts observed in the magnetic transitions.

The authors of Ref. 20 characterized their results as lending strong support for magnon-mediated pairing in the cuprates. Subsequent work has reported absence of an oxygen isotope effect (OIE) on T_N in $(\text{Ca}_x\text{La}_{1-x})(\text{Ba}_{1.75-x}\text{La}_{0.25+x})\text{Cu}_3\text{O}_y$ with oxygen content $y < 6.6$ (where T_N is independent of y),⁵³ indicating that the magnetic ordering is independent of isotopic substitution. Together with the presumed OIE on T_C (e.g., the comparison with Pr-doped $\text{YBa}_2\text{Cu}_3\text{O}_{7-\delta}$ in Ref. 53), this finding clearly disconnects magnetism from superconductivity in $(\text{Ca}_x\text{La}_{1-x})(\text{Ba}_{1.75-x}\text{La}_{0.25+x})\text{Cu}_3\text{O}_y$.

Implicit in the behavior observed is that magnetism accompanies sample degradation and suppression of superconductivity. It therefore seems reasonable to attribute these effects to increased pair

breaking, as defined by Eq. (4), in the underdoped regime, exclusive of any interdependency or symbiotic relationship between magnetism and superconductivity in $(\text{Ca}_x\text{La}_{1-x})(\text{Ba}_{1.75-x}\text{La}_{0.25+x})\text{Cu}_3\text{O}_y$. Although these magnetic studies are useful from the perspective of understanding the nonoptimal compounds, they shed limited light on the properties of the optimized superconducting condensate, which is the focus of the present work.

V. CONCLUSIONS

Given the body of evidence from transition-width, resistivity, and μ^+ SR data (Figs. 2 and 3), it is clear that there exists only one optimal $(\text{Ca}_x\text{La}_{1-x})(\text{Ba}_{1.75-x}\text{La}_{0.25+x})\text{Cu}_3\text{O}_y$ stoichiometry; $x \approx 0.45 \pm 0.05$ and $y \approx 7.15 \pm 0.02$. This stoichiometry also corresponds to a precipitous decrease in dT_C/dP , indicating that optimization occurs at ambient pressure. By applying rule (2b), the fractional charge σ for optimal $(\text{Ca}_x\text{La}_{1-x})(\text{Ba}_{1.75-x}\text{La}_{0.25+x})\text{Cu}_3\text{O}_y$ (scaled to σ_0 for $\text{YBa}_2\text{Cu}_3\text{O}_{6.92}$) is obtained as $\sigma = [(1.75 - x)/2] \sigma_0$, which is the charge available for superconductive pairing between the nearest-neighbor Ba/LaO and CuO_2 layers (separated by an interaction distance ζ) and evaluates to $\sigma = 0.1482 \pm 0.0057$, including the uncertainty in the optimal x . Given the relative insensitivity of T_C to x in the range $0.40 \leq x \leq 0.50$ (with optimized y), averaging $(\ell\zeta)^{-1}$ for the two end points provides an average value for the optimal transition temperature of $T_{C0} = 82.3(4)$ K, which is in excellent agreement with the experimental value of 80.5 K presented in Figs. 1, 4 and 5, as well as the claimed T_C^{max} of 82 K in Ref. 2 and 81 K in Refs. 3 and 4.

The local maxima in transition temperature observed for $x < 0.4$ (tuned by adjusting y), while not reflective of optimal superconducting states (independently indicated in Fig. 5), do nevertheless provide insights into sample inhomogeneities and magnetic phenomenology in the underdoped region, specifically showing that (1) T_C is not proportional to the μ^+ SR depolarization rate σ_μ (Fig. 3) and (2) the magnetism observed, at least for severely oxygen-deficient samples, is unrelated to the superconductivity. Moreover, the pair-breaking formalism of Eq. (4) with a unique and intrinsic optimum T_{C0} is consistent with the observed variation of T_C with x .

Particularly enlightening information comes from XAS experiments,²⁹ which find a near-invariance of the charge per planar Cu and O (corresponding to a near-constant 2D carrier density in the cuprate planes)

as a function of x . Given that the μ^+ SR experiments conducted on $(\text{Ca}_x\text{La}_{1-x})(\text{Ba}_{1.75-x}\text{La}_{0.25+x})\text{Cu}_3\text{O}_y$ record a significant dependence between σ_μ and x (consistent with the x dependence of T_C from transport and susceptibility),⁶ the results of Ref. 29 imply that most (e.g., 88%) of the superconducting condensate measured by μ^+ SR (and other techniques) is external to the CuO_2 planes. This leaves the $(\text{Ba/La})\text{O}$ layers of the type I reservoir as the likely locus of the superconducting hole condensate, which is an assignment consistent with that considered for $\text{YBa}_2\text{Cu}_3\text{O}_{7-\delta}$, as discussed in Ref. 5.

With the addition of $(\text{Ca}_{0.45}\text{La}_{0.55})(\text{Ba}_{1.30}\text{La}_{0.70})\text{Cu}_3\text{O}_{7.15}$, the list of compounds which behave in a manner consistent with the theoretical expression of Eq. (1) has grown to 37 in number, from six different superconducting families.

ACKNOWLEDGMENTS

We are grateful for the support of the Physikon Research Corporation (Project No. PL-206) and the New Jersey Institute of Technology. We also thank Amit Keren for suggesting this problem. This work has been published in Physical Review B.⁵⁵

REFERENCES

* drh@physikon.net

- ¹ D. Goldschmidt, G. M. Reisner, Y. Direktovitch, A. Knizhnik, E. Gartstein, G. Kimmel, and Y. Eckstein, *Phys. Rev. B* **48**, 532 (1993).
- ² D. Goldschmidt, A. Knizhnik, Y. Direktovitch, G.M. Reisner, and Y. Eckstein, *Phys. Rev.* **52**, 12982 (1995); D. Goldschmidt, A.-K. Klehe, J. S. Schilling, and Y. Eckstein, *Phys. Rev. B* **53**, 14631 (1996). The latter includes dT_C/dP .
- ³ A. Knizhnik and A. N. Men, *J. Phys. Chem. Solids* **62**, 513 (2001).
- ⁴ A. Knizhnik, Y. Direktovich, G. M. Reisner, D. Goldschmidt, C. G. Kuper, and Y. Eckstein, *Physica C* **321**, 199 (1999).
- ⁵ D. R. Harshman, A. T. Fiory, and J. D. Dow, *J. Phys.: Condens. Matter* **23**, 295701 (2011); **23** 349501 (corrigendum) (2011).
- ⁶ A. Keren, A. Kanigel, J. S. Lord, and A. Amato, *Solid State Commun.* **126**, 39 (2003).
- ⁷ V. Z. Kresin and S. A. Wolf, *J. Supercond. Nov. Magn.* **25**, 175 (2012).
- ⁸ S. A. Wolf and V. Z. Kresin, *J. Supercond. Nov. Magn.* **25**, 165 (2012).
- ⁹ D. R. Harshman, J. D. Dow, and A. T. Fiory, *Philos. Mag.* **91**, 818 (2011).

- ¹⁰ It has been suggested by the authors of Ref. 9 that this charge carrier duality feature of high- T_C compounds is likely the origin of some of the seemingly conflicting experimental results.
- ¹¹ D. R. Harshman, J. D. Dow, and A. T. Fiory, *Phys. Rev. B* **77**, 024523 (2008); **80**, 136502 (2009).
- ¹² D. R. Harshman and A. T. Fiory, *J. Phys.: Condens. Matter* **24**, 135701 (2012)
- ¹³ D. R. Harshman and A. T. Fiory, *Emerging Materials Research* **1**, 4 (2012).
- ¹⁴ W. Barford and J. M. F. Gunn, *Physica C* **156**, 515 (1988).
- ¹⁵ Results for σ_μ in anisotropic powder samples are discussed, e.g., in Ref. 16.
- ¹⁶ D. R. Harshman and A. T. Fiory, *J. Phys.: Condens. Matter* **23**, 315702 (2011).
- ¹⁷ E. H. Brandt, *Phys. Rev. Lett.* **66**, 3213 (1991).
- ¹⁸ E. H. Brandt, *Rep. Prog. Phys.* **58**, 1465 (1995).
- ¹⁹ P. A. Lee, N. Nagaosa, and X.-G. Wen, *Rev. Mod. Phys.* **78**, 17 (2006).
- ²⁰ R. Ofer, G. Bazalitsky, A. Kanigel, A. Keren, A. Auerbach, J. S. Lord, and A. Amato, *Phys. Rev. B* **74**, 220508(R) (2006).
- ²¹ R. Ofer, A. Keren, O. Chmaissem, and A. Amato, *Phys. Rev. B* **78**, 140508(R) (2008).
- ²² E. Amit and A. Keren, *Phys. Rev. B* **82**, 172509 (2010).
- ²³ P. Zimmermann, H. Keller, S. L. Lee, I. M. Savić, M. Warden, D. Zech, R. Cubitt, E. M. Forgan, E. Kaldis, J. Karpinski, and C. Krüger, *Phys. Rev. B* **52**, 541 (1995).
- ²⁴ S. Sanna, F. Coneri, A. Rigoldi, G. Concas, and R. De Renzi, *Phys. Rev. B* **77**, 224511 (2008).
- ²⁵ S. Yu. Gavrillkin, O. M. Ivanenko, V. P. Martovitskii, K. V. Mitsen, and A.Yu. Tsvetkov, *Physica C* **470**, s996 (2010).
- ²⁶ J. L. Tallon, C. Bernhard, and C. Niedermayer, *Supercond. Sci. Technol.* **10**, A38 (1997).
- ²⁷ Y. J. Uemura, *Physica B* **404**, 3195 (2009).
- ²⁸ J. A. Wilson, *J. Phys.: Condens. Matter* **22** 203201 (2010).
- ²⁹ S. Sanna, S. Agrestini, K. Zheng, R. De Renzi, and N. L. Saini, *Europhys. Lett.* **86**, 67007 (2009).
- ³⁰ Rule (2a) was defined specifically to apply to +3 cations such as Bi^{+3} mapped to the Cu^{+2} of the $\text{YBa}_2\text{Cu}_3\text{O}_{6.92}$ chain layers (partial substitutions are treated with the factor of 1/2 multiplying only the +3 ion component). In general, however, there are other possibilities of practical interest: For the type I central layers, one might also have a +1 ion mapped onto the Cu^{+2} , which is the logical corollary to the original. The -2 ion in rule (2b) typically refers to oxygen as in the case of $\text{YBa}_2\text{Cu}_3\text{O}_{6.6}$ (see Ref. 5).
- ³¹ The uncertainties in the (fitted) $k_B^{-1}\beta$ and T_{C0} values are obtained by assigning a 1-K experimental error bar for all data points (including $(\text{Ca}_{0.45}\text{La}_{0.55})(\text{Ba}_{1.30}\text{La}_{0.70})\text{Cu}_3\text{O}_y$), except for $\text{Ba}_2\text{Y}(\text{Ru}_{0.9}\text{Cu}_{0.1})\text{O}_6$ for which the error bar is set at 5 K.
- ³² V. Z. Kresin, A. Bill, S. A. Wolf, and Yu. N. Ovchinnikov, *Phys. Rev. B* **56**, 107 (1997).

- ³³ M. R. Presland, J. L. Tallon, R. G. Buckley, R. S. Liu, and N. E. Flower, *Physica C* **176**, 95 (1991).
- ³⁴ J. L. Tallon, C. Bernhard, H. Shaked, R. L. Hitterman, and J. D. Jorgensen, *Phys. Rev. B* **51**, 12911 (1995).
- ³⁵ A. Keren, A. Kanigel, and G. Bazalitsky, *Phys. Rev. B* **74**, 172506 (2006).
- ³⁶ T. Honma and P. H. Hor, *Phys. Rev. B* **75**, 012508 (2007).
- ³⁷ Variation of T_C with Cu-O spacing ($a/2$) is considered in Ref. 29. From the perspective of Eq. (1), reducing x from 0.4 to 0.1 increases a by 0.84 % and ζ by 6.27 % (Ref. 1), yielding a 7.06 % decrease in T_C which is significantly less than the 40 % observed.
- ³⁸ J. J. Scholtz, E. N. van Eenige, R. J. Wijngaarden, and R. Griessen, *Phys. Rev. B* **45**, 3077 (1992).
- ³⁹ F. Tao, G. C. Che, G. D. Liu, Z. X. Zhao, F. Wu, H. Chen, S. L. Jia, and C. Dong, *J. Alloys Compounds* **290**, 298 (1999).
- ⁴⁰ M. Izumi, T. Yabe, T. Wada, A. Maeda, K. Uchinokura, S. Tanaka, and H. Asano, *Phys. Rev. B* **40**, 6771 (1989).
- ⁴¹ The value of $y = 6.85$ corresponds to a pure stoichiometric $\text{LaBa}_2\text{Cu}_3\text{O}_y$ sample exhibiting the highest $T_C = 93$ K at the time of Ref. 40.
- ⁴² S. Kamal, R. Liang, A. Hosseini, D. A. Bonn, and W. N. Hardy, *Phys Rev B* **58**, R8933 (1998).
- ⁴³ V. Z. Kresin, Y. N. Ovchinnikov, and S. A. Wolf, *Phys. Repts.* **431**, 231 (2006).
- ⁴⁴ J. P. Carbotte, K. A. G. Fisher, J. P. F. LeBlanc, and E. J. Nicol, *Phys. Rev. B* **81**, 014522 (2010).
- ⁴⁵ T. M. Rice, K.-Y. Yang, and F. C. Zhang, *Repts. Prog. Phys.* **75**, 016502 (2012).
- ⁴⁶ Y. Imry, M. Strongin, and C. C. Homes, *Physica C* **468**, 288 (2008).
- ⁴⁷ C. C. Homes, *Phys. Rev. B* **80**, 180509(R) (2009).
- ⁴⁸ J. L. Tallon, J. W. Loram, J. R. Cooper, C. Panagopoulos, and C. Bernhard, *Phys. Rev. B* **68**, 180501(R) (2003).
- ⁴⁹ The curved trend of the data in Ref. 6 was misconstrued therein to be a proportional relationship.
- ⁵⁰ G. Drachuck, M. Shay, G. Bazalitsky, R. Ofer, Z. Salman, A. Amato, C. Niedermayer, D. Wulferding, P. Lemmens, and A. Keren, *J. Supercond. Nov. Magn.* **25**, 2331 (2012).
- ⁵¹ B. Watkins, H. Chashka, Y. Direktovich, A. Knizhnik, and Y. Eckstein, *Physica C* **449**, 57 (2006).
- ⁵² A. Kanigel, A. Keren, Y. Eckstein, A. Knizhnik, J. S. Lord, and A. Amato, *Phys. Rev. Lett.* **88**, 137003 (2002).
- ⁵³ E. Amit, A. Keren, J. S. Lord, P. King, *Adv. in Condens. Mat. Phys.* **2011**, 178190 (2011); this work compares $(\text{Ca}_x\text{La}_{1-x})(\text{Ba}_{1.75-x}\text{La}_{0.25+x})\text{Cu}_3\text{O}_y$ to Pr-doped $\text{YBa}_2\text{Cu}_3\text{O}_{7-\delta}$, the latter having been treated also in Ref. 11.
- ⁵⁴ A. Bill, V. Z. Kresin, and S. A. Wolf, *Phys. Rev. B* **57**, 10814 (1998).
- ⁵⁵ [D. R. Harshman and A. T. Fiory, Phys. Rev. B **86**, 144533 \(2012\).](#)